Received: 11 May 2020 | Revised: 2 July 2020 | Accepted: 5 July 2020

DOI: 10.1111/ffe.13303

ORIGINAL CONTRIBUTION

FFEMS Fatigue & Fracture of Engineering Materials & Structures WILEY

Thermodynamic entropy as a marker of high-cycle fatigue damage accumulation: Example for normalized SAE 1045 steel

Zhenjie Teng[1,2] | **Haoran Wu**[1,2] | **Christian Boller**[1] | **Peter Starke**[1,2]

[1]Chair of Non-Destructive Testing and Quality Assurance, Saarland University, Saarbrücken, Germany

[2]Department of Materials Science and Materials Testing, University of Applied Sciences Kaiserslautern, Kaiserslautern, Germany

Correspondence
Zhenjie Teng, Chair of Non-Destructive Testing and Quality Assurance, Saarland University, Saarbrücken, Germany.
Email: zhenjie.teng@hs-kl.de

Funding information
China Scholarship Council; Deutsche Forschungsgemeinschaft, Grant/Award Number: STA 1133/6-1

Abstract

A nondestructive thermographic methodology is utilized to determine the fracture fatigue entropy for evaluating the fatigue damage in metals within the high-cycle fatigue regime. Thermodynamic entropy is shown to play an important role in the fatigue process to trace the fatigue damage as an irreversible degradation of a metallic material being subjected to cyclic elastic-plastic loading. This paper presents a method to evaluate fatigue damage in the normalized SAE 1045 steel being based on the concept of thermodynamic entropy and its nonlinearities. The procedure looks to be applicable to constant and load increase tests proven by experiments.

KEYWORDS

damage accumulation, fatigue damage, high-cycle fatigue, thermodynamic entropy

1 | INTRODUCTION

Components in engineering are susceptible to fatigue and fracture if they are subjected to cyclic loads under operating conditions, which can lead to reduced usage or, in the worst case, to failure if threshold values are exceeded. In particular, the evaluation of the cumulative fatigue damage during the operation of those components and systems with regard to the prediction of fatigue life or for monitoring the integrity plays a decisive role.[1] Due to accumulation, fatigue damage increases with an increasing number of load cycles and ultimately leads to failure, whereby the time between damage initiation and failure depends on the load level, the type of load, the environmental conditions and possibly other factors.

The fatigue damage of metals comprises four stages,[2] including the following:

- Formation of dislocations and persistent slip bands.
- Nucleation of dislocations with the transition to micro-cracks.
- Micro-cracks direction perpendicular and then towards the maximum shear stress.
- Formation of the macro-cracks resulting in the generation of high stress intensities at the crack tips.

Moreover, the final stage includes the propagation of macro-cracks leading finally to fracture and a separation of the specimens into two parts.

From the view of continuum damage mechanics (CDM), fatigue damage is a process of accumulation that once reaches a critical state, the structural elements contain failures and cannot be serviced. Being able to grasp

[Correction added on 25 August 2020 after initial online publication. Projekt DEAL funding statement has been added.]

this damage accumulation allows a structure's remaining life to be assessed and even as a warning of the imminent failure that could be considered in the context of structural health monitoring (SHM).[3] In recent decades, many different models have been proposed for evaluating fatigue damage, whereby the following variables can be classified:

- Change in dynamic response (i.e., stress and strain).[4,5]
- Change in mechanical properties (i.e., elastic modulus, hardness, tensile strength and reduction area).[4,6–8]
- Change in physical properties (i.e., thermal, electric and magnetic properties).[4,9]

Those approaches are mostly derived from the theories of creep or plastic damage: there is always a margin for the improvement to make them more exquisite, and this is what should be discussed. The classic and most commonly used model is the Palmgren-Miner (P-M) rule,[10] which is characterized by its simplicity and can be written as follows:

$$D = \sum_{i=1}^{k} \frac{n_i}{N_i}, \tag{1}$$

where n_i and N_i are the number of cycles at a given stress amplitude and the lifetime at the same stress amplitude from the corresponding S-N curve, respectively. Damage D accumulates continuously starting from a pristine condition with $D = 0$ and reaches $D = 1$ when the component fails. The quality of the residual life assessment with this rule very much depends on the parameter describing the fatigue life curve. Traditionally, this parameter has been stress or strain only. However, more complex combinations such as those proposed by Smith et al,[11] Morrow[12] or Vormwald[13] are examples on how effects generating from notches, mean stresses, load sequence effects or others can be considered as well. Much of this can be found in textbooks such as Schijve,[2] Haibach[14] and Radaj and Vormwald.[15] Still, the damage parameter D can vary by a factor of 2 or more being the result of a variety of other material intrinsic effects not covered so far by parameters nor possibly monitored by any sensing device. Much research work has been done in that regard including many nonlinear stress-dependent cumulative damage theories such as to be found in other studies,[5, 16–20] where the accumulated damage versus the stress amplitude applied follows an exponential growth. The results obtained by the classic P-M rule are often overestimated when compared with nonlinear models or experimentally obtained data.

In order to improve the prediction of damage accumulation processes, various physically based measurement methods can be used, which can also be assigned to the field of nondestructive testing. In this context, temperature measurement in particular provides parameters that can be used to evaluate the fatigue-related damaging behaviour of metallic materials. As the damage can be an energy dissipative process, it must obey the laws of thermodynamics fundamentally related to an entropy approach.[21] In general, the fatigue mechanisms of a specimen or component are the result of irreversible thermodynamic processes taking place in the specimen or component during damage evolution. Degradation is a time-dependent index with the increasing disorder.[22] Thus, a basic parameter of thermodynamics is entropy, which can be derived from temperature measurements and can describe the degradation of the material due to fatigue loading.

Classical and statistics-based methods derived from entropy have been proposed to evaluate the fatigue damage as well as the remaining lifetime of materials and structures.[23–26] The accumulation of entropy generated during a fatigue test is calculated and regarded as a material property named the fatigue fracture entropy (FFE), where this parameter stays constant for a certain material until failure. This parameter is moreover independent of loading sequences, frequency, amplitudes, and so forth,[27] and affects the fatigue such as damage evaluation,[28] temperature response,[29] and reliability[30] of the material. However, those FFE calculation models have not taken the evolution of temperature variation entropy before final facture into account, which should be much higher than in the initial phase.

In the work presented here, the FFE approach has been modified and used as an index of degradation to monitor fatigue damage for the normalized SAE 1045 steel. The approach is based on temperature measurements carried out during constant amplitude and variable amplitude loading tests in the high-cycle fatigue regime. The experimental procedure is presented below followed by a methodology being related to damage accumulation based on the concept of the thermodynamic entropy. The results obtained are discussed with regard to the concept of entropy under plastic deformation, and conclusions are finally drawn.

2 | EXPERIMENTAL PROCEDURE

2.1 | Material

The material used in this study is the unalloyed medium carbon steel SAE1045 (German-standard: C45E), which is in accordance to DIN EN 10083-1. The requested and manufacturer-determined chemical compositions and the material properties are listed in Tables 1 and 2, respectively.

TABLE 1 Chemical compositions of normalized SAE 1045

(Wt.-%)		C	Si	Mn	P	S	Cr	Mo	Ni
DIN	Min	0.42	-	0.50	-	-	-	-	-
	Max	0.50	0.40	0.80	0.030	0.035	0.40	0.10	0.40
Customer's report		0.47	0.23	0.72	0.012	0.013	0.06	0.014	0.07

TABLE 2 Material properties of normalized SAE 1045

Property	Unit	Value	Property	Unit	Value
Ultimate strength	MPa	710	Mass density	Kg m^{-3}	7,821
Yield strength	MPa	413	Specific heat capacity	J kg^{-1} K^{-1}	474
Poisson's ratio	—	0.3	Heat conduction coefficient	W m^{-1} K^{-1}	48
Young's modulus	GPa	214	Linear thermal expansion coefficient	10^{-6} K^{-1}	11
Brinell hardness	HB	210			

Note. Thermophysical parameters taken from the Spittel and Spittel.[56]

2.2 | Fatigue testing

Tension-compression fatigue tests were performed using a servo-hydraulic fatigue testing system (Shimadzu EHF-L) with a 20/25 kN cyclic/quasi-static load capacity as shown in Figure 1 and run at a loading frequency of 5 Hz and a stress ratio of $R = -1$, respectively. Temperature measurement areas (10 × 10 pixels) defined on the specimens' surface were recorded by using an infrared camera (Micro-Epsilon thermoIMAGER TIM 245) with a resolution of 382 × 288 pixels in the full window mode and at a thermal sensitivity of 0.04 K at room temperature and with a 100-Hz recording frequency in order to avoid too large data volumes. The cylindrical hourglass specimen was designed with an arc radius of 30 mm and a minimum diameter in the gauge length of 5.8 mm, and the surface of the specimen was coated with a thin layer of matt black paint for having a high and uniform thermal emissivity.

The fatigue tests were carried out in load control mode with a sinusoidal waveform and a stress function to be expressed as $\sigma(t) = \sigma_a \sin(10\pi t)$. In order to evaluate the processes of fatigue damage evolution, two types of fatigue tests were performed: the one being a constant amplitude and the other a load increase test, respectively. The details of the respective load types for the tests performed are summarized as follows:

- Constant amplitude tests: five tests at stress amplitudes between 320 and 400 MPa, with each test differing in 20 MPa of stress amplitude.
- Load increase tests: all tests starting from a stress amplitude level of $\sigma_{a,start}$= 100 MPa, being below the fatigue strength, σ_f= 300 MPa,[31] of the normalized

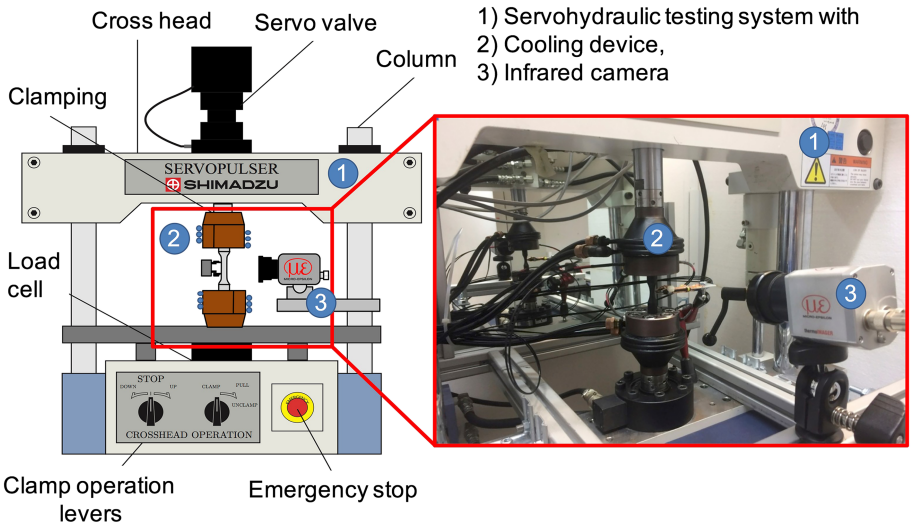

FIGURE 1 Experimental setup with servo-hydraulic fatigue test system and thermographic measurement [Colour figure can be viewed at wileyonlinelibrary.com]

SAE 1045 steel investigated at $R = -1$ and being loaded for a defined number of cycles ΔN before increasing the stress amplitude by an increment $\Delta\sigma_a$ to a next stress amplitude level while cycling again the specimen with a number ΔN of cycles and this to be continued so forth until the specimen failed. A distinction has been made between tests in which (a) ΔN was retained constant at 9,000 cycles and $\Delta\sigma_a$ increased in steps of 5 MPa from 20 to 40 MPa as well as in tests where (b) $\Delta\sigma_a$ was kept at 25 MPa and ΔN was varied to step lengths of 1000, 2000, 3000, 4500 and 6000 cycles, respectively.

3 | METHODOLOGY

3.1 | First law of thermodynamics

The first law of thermodynamics describes the energy balance status, which can be applied to every thermomechanical process. For a defined volume of material under load such as the volume of a fatigue specimen in its minimum cross-section, this can be formulated as follows:

$$\Delta U = Q + W, \tag{2}$$

where ΔU indicates the change of the internal energy, Q is the thermal energy dissipated as heat and W is the work applied to deform the material under elastic-plastic conditions. For a given quantity term, Equation 2 can be formulated as follows:

$$\rho\dot{u} = \boldsymbol{\sigma} : \dot{\boldsymbol{\varepsilon}} - \mathrm{div}J_q, \tag{3}$$

where u denotes the specific internal energy, $\boldsymbol{\sigma}$ is the Cauchy stress tensor, $\dot{\boldsymbol{\varepsilon}}$ is the Eulerian strain rate tensor and J_q is the heat flux vector. The term $\boldsymbol{\sigma} : \dot{\boldsymbol{\varepsilon}}$ is the stress power for uniaxial cyclic loading expressed as $\boldsymbol{\sigma} : \dot{\boldsymbol{\varepsilon}} = \sigma : \left(\dot{\varepsilon}_e + \dot{\varepsilon}_p\right)$, where ε_e and ε_p are the elastic and plastic strain portions, respectively.

The heat flux, internal energy, entropy and Cauchy stress are the state functions in thermodynamics. For an ideal thermoelastic state, those parameters are a function of the deformation and the temperature state variables.[32] However, if the deformation is in the inelastic state, the situation is more complex and the internal state variables, such as mechanical, thermal and electrical, in the history of deformation sequence need to be considered.

Furthermore, those variables can be associated with defects in a material such as dislocations or voids in the materials' microstructure.[33]

The Helmholtz free energy is defined as a part of the internal energy of a system and can be expressed as follows:

$$\psi = u - T\gamma, \tag{4}$$

where T is the temperature and γ is the entropy per unit volume. The Helmholtz free energy ψ is considered as a function of temperature and multiple internal state variables[34] and can be stated as follows:

$$\psi = \psi\left(\varepsilon_e, T, V_k\right), \tag{5}$$

where V_k is introduced as a set of internal state variables. Following this, the rate of free energy can be developed as follows:

$$\dot{\psi} = \frac{\partial\psi}{\partial\varepsilon_e} : \dot{\varepsilon}_e + \frac{\partial\psi}{\partial T} : \dot{T} + \frac{\partial\psi}{\partial V_k} : \dot{V}_k. \tag{6}$$

By using the thermoelastic relationships valid for small strains, where $\sigma = \frac{\partial\psi}{\partial\varepsilon_e}$ and $\gamma = -\frac{\partial\psi}{\partial T}$, and further substituting Equations 4 and 6 in 3, the thermodynamic energy balance equation can be written as follows:

$$\rho c_p \dot{T} = \sigma : \dot{\varepsilon}_p - \mathrm{div}J_q + T\frac{\partial\sigma}{\partial T} : \dot{\varepsilon}_e + \left(A_k - T\frac{\partial A_k}{\partial T}\right)\dot{V}_k, \tag{7}$$

where $c_p = \frac{T}{\rho}\frac{\partial\gamma}{\partial T}$ represents the heat capacity, $A_k = -\frac{\partial\psi}{\partial V_k}$, where A_k is the thermodynamic force associated with the internal variables and k is the heat conductivity and ρ is the materials' density. $\rho c_p \dot{T}$ is the rate of the change in internal energy. $\sigma : \dot{\varepsilon}_p$ is the heat generation due to the plastic deformation and symbolized as w_p, $\mathrm{div}J_q$ is the heat transfer by conduction, $T\frac{\partial\sigma}{\partial T} : \dot{\varepsilon}_e$ is the thermoelastic coupling and $\left(A_k - T\frac{\partial A_k}{\partial T}\right)\dot{V}_k$ is related to the internal state variables. Thus, the mean temperature rise within the specimen's gauge length section is related to the plastic strain energy term and the thermoelastic effect to the thermoelastic coupling term, whereby tension results in a decrease and compression in an increase in the temperature, respectively.[32]

3.2 | Second law of thermodynamics

The second law of thermodynamics (Clausius-Duhem inequality), which is applied to a specimen subjected to fatigue, is generally written as follows:

$$\dot{s} = \mathrm{div}\left(\frac{J_q}{T}\right) + \rho\dot{\gamma}, \tag{8}$$

and can be further developed as

$$\dot{s} = \rho\dot{\gamma} + \frac{J_q}{T} - \left(\frac{J_q}{T^2}\cdot\nabla T\right) \geq 0, \tag{9}$$

where $\dot{s}$ is the entropy generation rate resulting from the irreversibility of thermodynamic transformation. The use of the first law of thermodynamics (Equation 3) and the Helmholtz free energy (Equation 4) applied to the second law of thermodynamics (Equation 8) leads to

$$\dot{s} = \frac{\sigma:\dot{\varepsilon}}{T} - \frac{\rho}{T}\left(\dot{\psi} + \gamma\dot{T}\right) - \left(\frac{J_q}{T^2}\cdot\nabla T\right) \geq 0. \tag{10}$$

Combining Equations 6 and 10 and using $\varepsilon_p = \varepsilon - \varepsilon_e$ as a simplification due to a small strain assumption in the case of high-cycle fatigue, the specific entropy generation flow can be expressed as follows:

$$\dot{s} = \frac{\sigma:\dot{\varepsilon}_p}{T} - \frac{A_k\dot{V}_k}{T} - \left(\frac{J_q}{T^2}\cdot\nabla T\right) \geq 0, \tag{11}$$

where[35]:

- $\frac{\sigma:\dot{\varepsilon}_p}{T}$ is the specific entropy generation derived from plastic deformation.
- $-\frac{A_k\dot{V}_k}{T}$ is the specific entropy generation caused by irreversible deformation, such as strain hardening and phase transformation.
- $\frac{J_q}{T^2}\cdot\nabla T$ is the specific entropy generation provided through heat conduction.

Therefore, the entropy generation accumulation can be obtained by integrating Equation 11 as follows:

$$s = \int_0^t \dot{s}dt. \tag{12}$$

Thus, the FFE, namely the maximum entropy generation at the onset of fracture generated by irreversibility during the fatigue process, is $s_f = \int_0^{t_f}\dot{s}\,dt$, where t_f is the time to failure. In the case of materials with low hardening potential and at sufficiently high fatigue test frequencies, the second and the third terms of Equation 11 can be neglected as it was proposed in[35] the following:

$$\left|\frac{A_k\dot{V}_k}{T}\right| \ll \left|\frac{\sigma:\dot{\varepsilon}_p}{T}\right|, \quad \left|\frac{J_q}{T^2}\cdot\nabla T\right| \ll \left|\frac{\sigma:\dot{\varepsilon}_p}{T}\right|. \tag{13}$$

In this case, the generated entropy can be simplified as follows:

$$s_f = \int_0^{t_f}\frac{\sigma:\dot{\varepsilon}_p}{T}\,dt. \tag{14}$$

The cyclic plastic strain energy generation per second, $W_p = \sigma:\dot{\varepsilon}_p$, can be expressed by an empirical relation, which was originally proposed by Morrow[36] as follows:

$$W_p = 2^{2+b+c}\sigma'_f\varepsilon'_f\left(\frac{c-b}{c+b}\right)N_f^{b+c}, \tag{15}$$

where b and c are the fatigue strength exponent and the fatigue ductility exponent, respectively, σ'_f is the fatigue strength coefficient, ε'_f is the fatigue ductility coefficient and N_f is the number of cycles to failure. The above-mentioned relation can be further used to evaluate the entropy generation rate.[24,26,37] The constant W_p is given as a default constant, since the above parameters are determined constantly for a fatigue test. However, numerous studies[38–47] have shown that the temperature evolution of a specimen or a component that had been exposed to a load amplitude higher than its fatigue limit appears in three stages, which is schematically represented in Figure 2. This can be divided into an initial temperature increase (Stage 1), a predominant temperature stabilized stage (Stage 2) and a sudden temperature increase stage close before fracture (Stage 3). What needs to be addressed is that the entropy generation rate in the first stage cannot be higher than in the second stage and then in the third, respectively. To circumvent this disadvantage and to modify the entropy calculation, a method for evaluating W_p based on intrinsic dissipation is presented in the following sections.

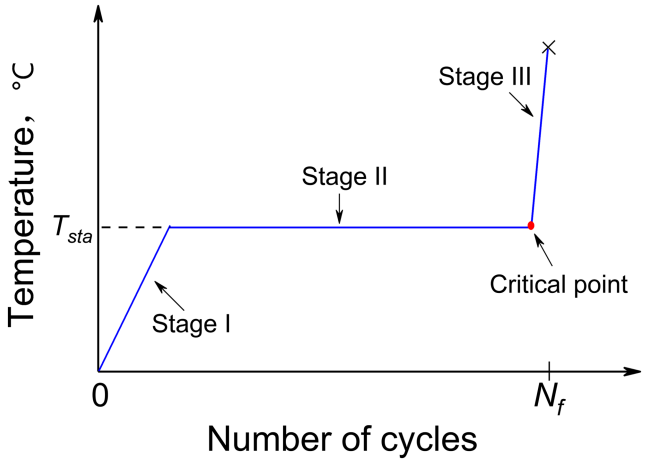

FIGURE 2 Schematic representation of the temperature evolution process during a single loading stage [Colour figure can be viewed at wileyonlinelibrary.com]

3.3 | Intrinsic dissipation

Following the laws of thermodynamics, Boulanger et al[48] proposed a specific form of heat diffusion of a local heat by measuring the temperature fields of the surface of a specimen during fatigue tests which are formulated as follows:

$$\rho c_p \dot{\theta} - \mathrm{div}(k : \mathrm{grad}\theta) = s_{the} + s_i + d_1 + r_{ext}, \tag{16}$$

where c_p is the heat capacity, $\theta = T - T_0$ is the change in temperature with T_0 being the equilibrium temperature and k is the thermal conductivity. On the right-hand side of Equation 16, s_{the} indicates the thermoelastic source term, s_i is the internal coupling source term, d_1 is the intrinsic dissipation term and r_{ext} is the heat exchange between the specimen and the surroundings, respectively.

For the fatigue tests were performed at room temperature, the external heat source r_{ext} denotes the heat loss into the environment and it can be influenced by conduction, convection and radiation. Those elements are very hard to be accurately estimated as they strongly depend on the boundary conditions of the test setup. Normally, it is supposed to be a simple time-independent and linear-solution[49] as follows:

$$r_{ext} = -\rho c_p \frac{\theta}{\tau_{eq}}, \tag{17}$$

where τ_{eq} represents a time constant characterizing the heat loss. Here, it is assumed that the change in temperature during the high-cycle fatigue tests do not influence the microstructure, and then the internal coupling source s_i can be neglected under the given boundary condition because the thermal process due to fatigue is considered as a pure dissipation mechanism. Considering the 0D heat diffusion model is used in the present case, then Equation 16 can be further simplified as follows:

$$\rho c_p \left(\frac{\partial \theta}{\partial t} + \frac{\theta}{\tau_{eq}} \right) = d_1 + s_{the}. \tag{18}$$

In the fully reversed tension-compression fatigue test, the thermoelastic source s_{the} turns out to be zero after each loading cycle due to the cyclic load mode, and the temperature variation tends to be asymptotic with $\dot{\theta} = 0$. According to the above estimates, the dissipated energy within a time unit can be simplified as follows[48,50]:

$$d_1 = \rho c_p \frac{\theta}{\tau_{eq}}. \tag{19}$$

3.4 | A unified entropy approach

According to the energy balance principle, the dissipated energy takes up most of the plastic energy generated during cyclic loading but not all. The remaining portion is stored within the material as stored energy that takes part in the process of the microstructure evolution and results from micro defects, crystal lattice or dislocation structures, as well as possibly others.

This energy is described as stored energy E_s and is comparable with the stored energy of cold work associated with plastic deformation. The Taylor-Quinney coefficient[51,52] β is used to bridge between the fraction of plastic energy W_p and the dissipated energy E_d as follows:

$$\beta = \frac{W_p - E_s}{W_p} = \frac{E_d}{W_p}. \tag{20}$$

For metallic materials, studies have shown that approximately 80% to 100% of the plastic work dissipates as heat, leading to an increase in the specimen's temperature[49,50,53,54] and it is normally assumed β to be an independent material constant. For the material considered here, the intermediate value is adapted to $\beta = 0.9$.

The dissipated energy during one loading cycle can be integrated as follows:

$$E_d = \int_t^{t+\tau} d_1 \, dt, \tag{21}$$

where $\tau = 1/f$ indicates the period of one loading cycle. Substituting Equations 19, 20 and 21 into Equation 14, the entropy generation is obtained as follows:

$$s(t) = \frac{\rho c_p}{f \beta \tau_{eq}} \int_0^t \left(\frac{T - T_0}{T} \right) dt. \tag{22}$$

3.5 | Damage accumulation

Based on the theory of CDM, failure of the specimen occurs when the damage parameter reaches a critical value. Chaboche[16] defined this value as the breaking point of the continuum element, which is the point where fatigue damage results in the initiation of macro-cracks. Thus, the fatigue damage accumulation can be

regarded as a degradation of the material. A relationship between degradation caused by damage and entropy generation was proposed by Naderi[37] using degradation entropy generation, which is the following:

$$D = A + B \cdot \ln\left(1 - s/s_f\right), \tag{23}$$

where D is a damage parameter and A and B are material parameters, respectively.

Damage is initiated by slipping and then followed by slip bands, intrusions and extrusions, which result in micro-cracks, whereby different of the micro-cracks merge, leading to micro-cracks finally before a complete fracture occurs. Here, D_c is defined as the critical damage value, which corresponds to the onset of the macro-crack initiation, and s_c is the critical entropy generation value, which corresponds to the onset of the temperature rise at the beginning of the macro-crack initiation or before the complete failure. This critical condition is considered as an indication of an imminent fracture and could be used as a marker for the purposes of SHM. In addition, let s_0 be defined as the initial entropy generation value with respect to the initial damage of D_0 for a constant stress amplitude fatigue test, then Equation 23 yields to the following:

$$\begin{cases} D_0 = A + B \cdot \ln\left(1 - {}^{s_0}/_{s_f}\right) \\ D_c = A + B \cdot \ln\left(1 - {}^{s_c}/_{s_f}\right) \end{cases} \tag{24}$$

Solving A and B and substituting into Equation 23:

$$D = D_0 + \frac{D_c - D_0}{\ln\left[\left(1 - s_c/s_f\right)/\left(1 - s_0/s_f\right)\right]} \ln\left(\frac{1 - s/s_f}{1 - s_0/s_f}\right) \tag{25}$$

Equation 24 provides a relationship between damage evolution and the history effect of entropy generation. For constant amplitude tests, the initial damage is zero ($D_0 = 0$) with no entropy generated. Equation 25 can be simplified to the following:

$$D = \frac{D_c}{ln\left(1 - s_c/s_f\right)} ln\left(1 - s/s_f\right). \tag{26}$$

In engineering applications, most components are subjected to variable amplitude loading and hence should have 'entropy memory.' Then, Equation 25 can be further extended to an n-stage sequence as follows:

$$D_k = D_{k-1} + \frac{D_c - D_{k-1}}{\ln\left[\left(1 - s_c/s_f\right)/\left(1 - s_{k-1}/s_f\right)\right]} \ln\left(\frac{1 - s/s_f}{1 - s_{k-1}/s_f}\right), \text{ for } k = 1, 2, \ldots, n, \tag{27}$$

where D_{k-1} and s_{k-1} are the damage parameter and the accumulated entropy for (k-1)th stage, respectively.

The schematic principle for the fatigue damage evolution versus the number of cycles is shown in Figure 3 for load increase tests, where N_f is the number of cycles to failure and ($N_k - N_{k-1}$) is the number of cycles of the corresponding loading stage. During the fatigue process, the degradation progresses with the existing micro-cracks and the nucleation and propagation of the new micro-cracks. Meanwhile, the entropy generates due to the progressed irreversibility at each stage of loading. The degradation grows and the entropy accumulates from the beginning to the onset of the second stage. Similarly, the accumulated damage at the end of one loading stage is the initial damage of the next stage and the transition point is named as the knee point. The number of micro-cracks increases and the entropy increases as well. Finally, in the last stage, as soon as the macro-cracks once occur, the entropy and hence damage propagates exponentially perpendicular to the stress amplitude level and up to the final failure.

4 | RESULTS AND DISCUSSION

4.1 | Evolutions of entropy generation rate

The evolutions of the entropy generation rate at constant amplitude and load increase tests are given in Figures 4 and 5, respectively, for the normalized SAE 1045 steel. For the constant amplitude tests, the progress of the rate development is similar to the three-stage behaviour schematically shown in Figure 2.

During the first few thousand cycles, the entropy generation rate increases and then reaches a more stationary state with the rate development starting at zero. For the different stress amplitudes, the average rate drifts upwards with an increasing number of cycles until a steady state is achieved. With the exception of the stress amplitude of 400 MPa, the rate in Stage 2 is somewhat lower that may cause by cyclic hardening effects. There is no doubt that the stable mean entropy generation rate along the gauge of the specimen increases monotonically with increasing stress levels. Finally, the rate increases strongly due to the large plastic deformation caused by stress intensities at the crack tips.

For the load increase tests, the entropy generation rate remained close to zero at the beginning of the

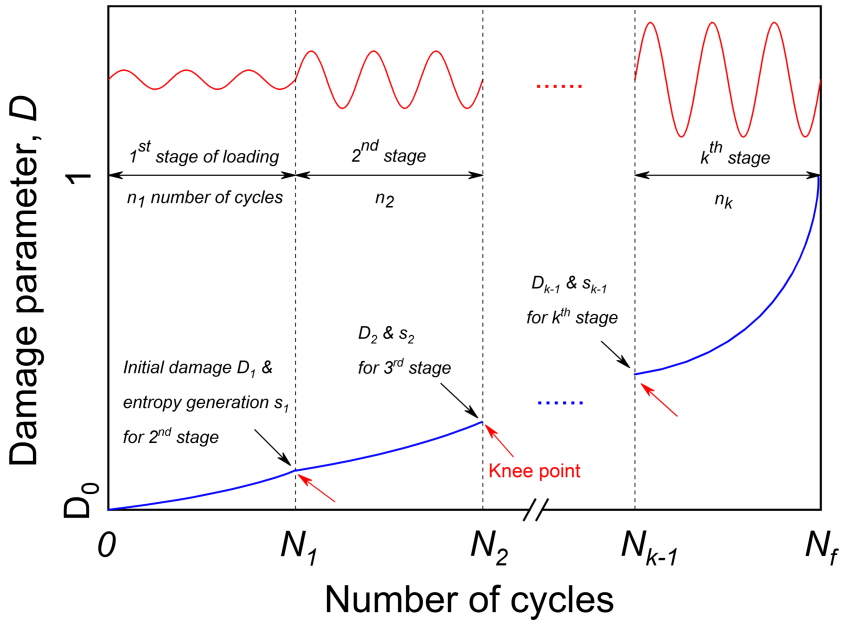

FIGURE 3 Schematic of damage accumulation versus number of cycles during load increase tests [Colour figure can be viewed at wileyonlinelibrary.com]

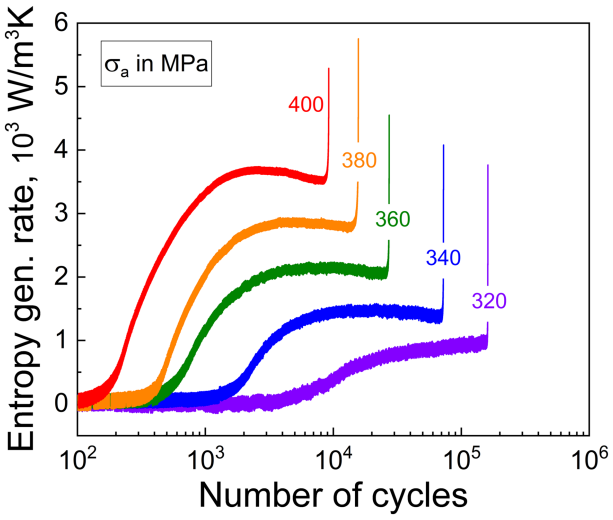

FIGURE 4 Entropy generation rate versus the number of cycles in the constant amplitude tests [Colour figure can be viewed at wileyonlinelibrary.com]

loading sequence, indicating that for stress amplitudes below the fatigue limit, fatigue damage due to the internal friction effect is not measurable,[55] shear stresses within the lattice structure are below a certain critical value and dislocation reactions, such as dislocation movement, the formation of walls or subgrains, are limited. When the stress amplitude is above the fatigue limit, zones of localized microplastic deformation emerge and dislocation reactions such as increase or decrease in dislocation density or movement appear. Those processes lead to an irreversible microstructural change and consequently to an increase in dissipated energy, which is reflected in the macroscopic appearance of the temperature.[50] The development of the entropy generation rate obviously shows an accelerated increase corresponding to the stepwise increased stress amplitudes and the first two stages can be observed while Stage 3 indicates the fracture of the specimen and is limited to the last loading sequence of the load increase test.

4.2 | Damage evolution in constant amplitude tests

Figure 6 shows the evolution of the damage parameter for the normalized SAE1045 steel at different stress amplitudes of the constant amplitude loading tests. The specimens have a low defect density at the beginning, where $D_0 = 0$. It can be clearly seen that in the early stages of the fatigue life, the damage parameter can be approximated to increase monotonically with the slope increasing continuously in a nonlinear way with an increasing number of cycles until final fracture. This development is different for the different stress amplitudes being applied as can be seen from the results shown in Figure 6. This further proves that the linear accumulation postulated in the P-M rule does not hold.

Figure 7 graphically presents the damage evolution versus normalized entropy generation (s/s_f) for different stress amplitudes. At the same normalized entropy level, the higher stress amplitudes result in higher values of the fatigue damage parameter. The discrepancy in the evolution of the damage parameter for the fatigue test with a stress amplitude of 400 MPa is due to cyclic hardening processes shown in Figure 4 and has, therefore, to be considered separately.

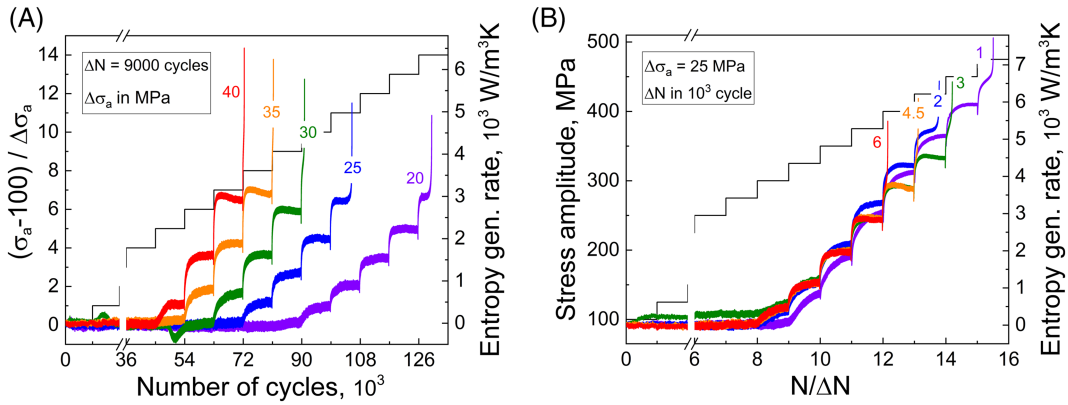

FIGURE 5 Entropy generation rate and stress amplitude versus the number of cycles of load increase tests: (A) in constant loading step length and (B) in constant load increments [Colour figure can be viewed at wileyonlinelibrary.com]

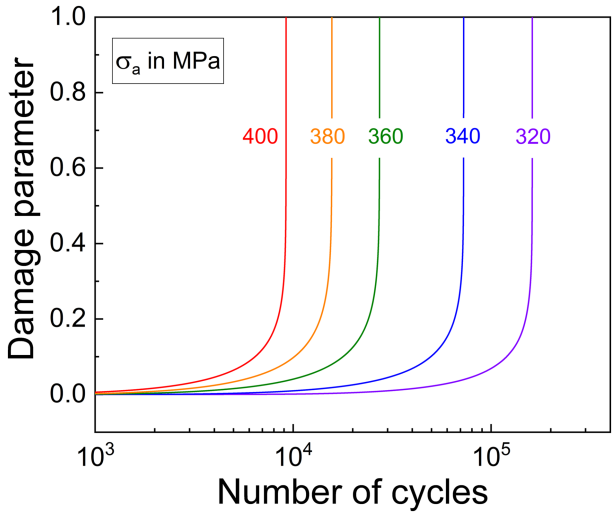

FIGURE 6 Damage parameter versus the number of cycles of constant amplitude tests [Colour figure can be viewed at wileyonlinelibrary.com]

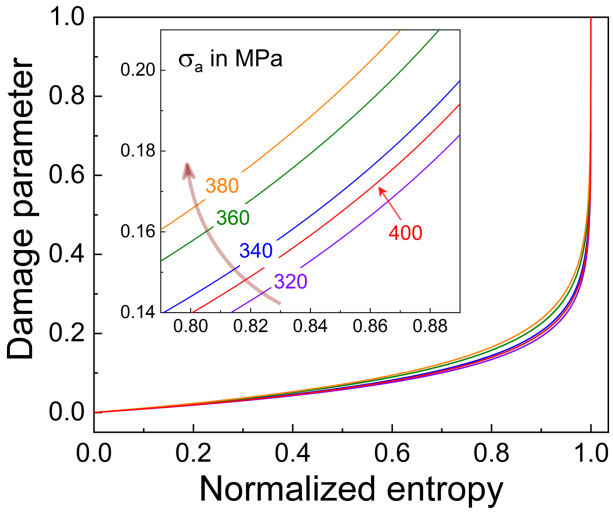

FIGURE 7 Damage parameter versus normalized entropy of constant amplitude tests [Colour figure can be viewed at wileyonlinelibrary.com]

According to Equation 26, the result shows a good relationship between fatigue degradation and entropy generation. It is therefore pointed out that thermodynamic entropy as an index of fatigue degradation can be used to assess the fatigue damage in the cyclic loading process.

4.3 | Damage evolution in load increase tests

A load increase test is an interesting experiment to study the entropy development at different stress levels within a single experiment. Using the fatigue damage equation and the entropy generation relationship, the evolution of the fatigue damage can be evaluated.

The damage evolution versus the fatigue life of the normalized SAE1045 steel exposed to the load increase sequence as described before is shown in Figure 8. In the unloaded state, the specimens show initially a low defect density, $D_0 = 0$, namely no micro-cracks or damage, and to be free from an entropy history expressed as $s_i = 0$. When the stress amplitudes are lower than the fatigue limit, no measurable fatigue damage is observed from the entropy information. Measurable degradation starts with the typical fatigue characteristics resulting from intrusions and extrusions that can be observed on a specimens' surface. Thereafter, micro-cracks start to nucleate and then move along the slip planes of maximum shear stress, which is in the case of uniaxial loading 45° related to the loading direction. The higher the stress amplitude is applied, the more sites of microplastic deformation are

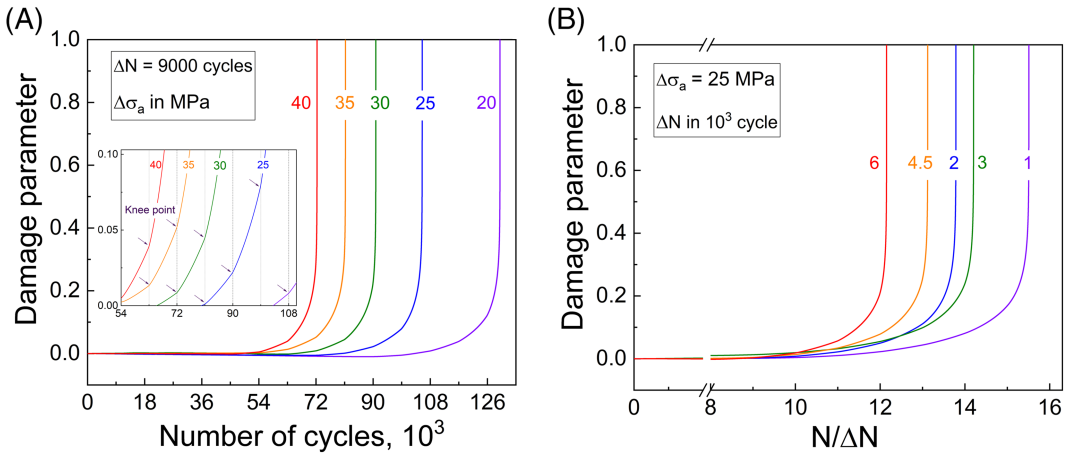

FIGURE 8 Damage parameter versus the number of cycles of the load increase tests: (A) in constant loading step length and (B) in constant load increments [Colour figure can be viewed at wileyonlinelibrary.com]

activated being a consequence of inconsistent grain boundaries, localized dislocations and inhomogeneous grain size. When the stress is higher than the fatigue limit, plastic deformation becomes measurable and the entropy progressively increases from load level to load level. It can be observed from Figure 5 that Stages 1 and 2 can be described for each loading level, and it is therefore logical to assume that what has been accumulated at the end of Stage 1 corresponds to the initial value of Stage 2 and being continued so forth. Thus, the rate of the degradation changes with the amount of stress being applied, which can be observed from the knee points indicated by arrows in Figure 8A. As the number of cycles increases, micro-cracks are nucleated and connected to form a macro-crack, which can be referred to as the critical damage through measurement of a critical entropy formation. Near the final failure, the damage size increases dramatically and the fracture occurs after the formation of macro-cracks with the fatigue damage parameter reaching the value of 1.

As discussed above, the entropy generation during the fatigue process can be used as an index to evaluate the fatigue degradation. Simultaneously with the rise of the degradation, the entropy continuously increases as well towards the final FFE. Based on former work, the FFE for a certain material is constant,[35,37] regardless of the type of the mechanical fatigue load, such as tension-compression, bending or torsion, frequency and geometry, and possibly others, which has been proven through the application of different models of FFE calculation.[27,35] Based on Equation 21, the results of FFE calculations for 15 specimens are given in Figure 9. The spreading of final test data is a bit large, excluding the two too high points, and the FFE for normalized SAE 1045 steel is about 8.6 MJ/m^{3}K. For a more precise fatigue damage calculation, the above used FFE data came from its own test instead of the average value. Besides, more load-history tests will be performed in the future to quantify the dispersion of the FFE of normalized SAE 1045 steel.

The evolution of fatigue damage versus the normalized entropy generation is depicted in Figure 10. As the damage progresses towards the final fatigue failure, the accumulated entropy increases monotonically until FFE. The agreement is very good, which can prove that FFE is independent of the load sequence. It should also be noted that the cumulative entropy generation gives a unit value that can be used as a criterion for the onset of fatigue damage or can be used with regard to SHM activities for detecting damage before final fracture.

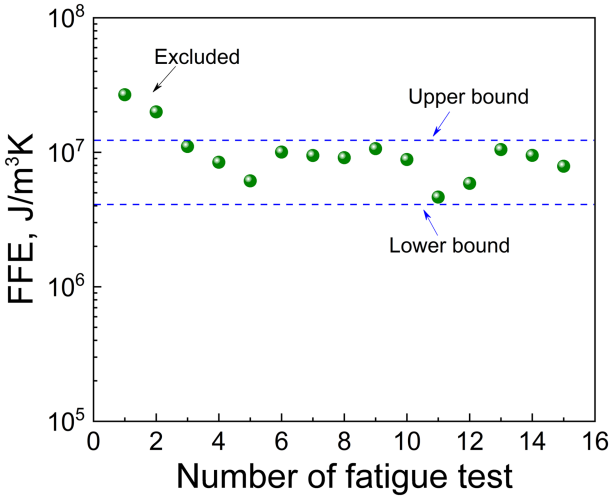

FIGURE 9 The values of fatigue fracture entropy of normalized SAE 1045 steel [Colour figure can be viewed at wileyonlinelibrary.com]

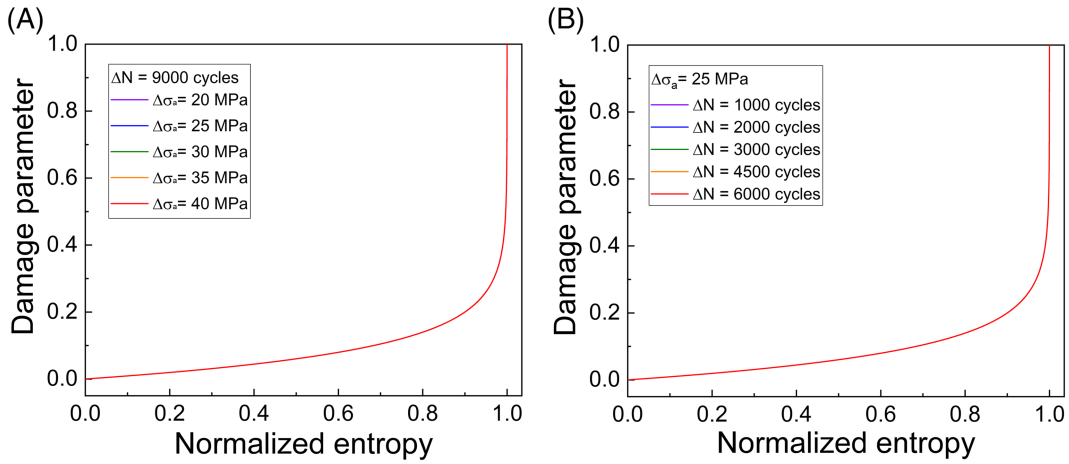

FIGURE 10 Damage parameter versus normalized entropy of load increase tests: (A) in constant loading step length and (B) in constant load increments [Colour figure can be viewed at wileyonlinelibrary.com]

5 | CONCLUSIONS

A modified approach based on thermodynamic entropy generation is an effective strategy for monitoring the development of fatigue damage, which has been verified through various constant amplitude and load increase tests. The evolution of the entropy generation rate during the fatigue testing can be well given based on this modified entropy calculation method. The tests were carried out at room temperature under stress-control and a stress ratio of $R = -1$. The material investigated was the unalloyed medium carbon steel SAE 1045 in the normalized condition, which is widely used for engineering components. Unlike the P-M rule, the proposed method takes the temperature or the FFE as an index of degradation, and a nonlinear equation is used to characterize the relationship between the degradation provided by damage and entropy generation. It can be seen from the results that the FFE is independent of the load-time history and can be calculated to a value of approximately 8.6 MJ/m^{3}K. As expected, there is an overestimation of the fatigue damage by using the linear P-M rule, which underlines the advantages of nonlinear damage accumulation approaches.

Another thermodynamic parameter, exergy, can also be used to evaluate fatigue damage since it considers the influence of the environment on the irreversibility of the thermodynamic system and the calculation process is similar to the entropy, which will be discussed in the future. In addition, the proposed approach still has to be subjected to a comprehensive experimental validation, whereby in addition to different stress amplitudes, also different load time histories have to be included in the verification, and even with different metals and alloys, or with heat-treatment procedures. Corresponding investigations are currently ongoing and will be continued within the framework of further research work.

ACKNOWLEDGEMENTS

This work was supported by the German Research Foundation (Deutsche Forschungsgemeinschaft DFG, STA 1133/6-1) and the China Scholarship Council. Open access funding enabled and organized by Projekt DEAL.

NOMENCLATURE

A_k	thermodynamic force
D_0	initial damage
D_c	critical damage
D_k	damage parameter at kth stage
D_{k-1}	damage parameter at (k-1)th stage
E_d	dissipated energy
E_s	stored energy
J_q	heat flux vector
N_f	number of cycles to failure
N_i	number of cycles to failure at stress amplitude σ_a
N_k	number of cycles at kth stage
N_{k-1}	number of cycles at (k-1)th stage
T_0	equilibrium temperature
V_k	internal state variables
W_p	plastic energy
c_p	heat capacity
d_1	intrinsic dissipation term
n_i	number of cycles at a given stress amplitude σ_a
r_{ext}	heat exchange
$\dot{s}$	entropy generation rate
s_0	initial entropy generation
s_c	critical entropy generation
s_f	maximum entropy generation
s_i	internal coupling source term
s_{k-1}	accumulated entropy at (k-1)th stage

s_{the}	thermoelastic source term
t_f	time to failure
$\dot{\boldsymbol{\varepsilon}}$	Eulerian strain rate tensor
ε_e	elastic strain
ε'_f	fatigue ductility coefficient
ε_p	plastic strain
σ_{f}	fatigue strength
σ'_f	fatigue strength coefficient
τ_{eq}	time constant
$\Delta\sigma_a$	load increase step
ΔN	load step length
ΔU	change in internal energy
T	temperature
A	material parameter
B	material parameter
D	damage variable
Q	heat dissipation
R	stress ratio
W	mechanical work
b	fatigue strength exponent
c	fatigue ductility exponent
f	frequency
k	heat conductivity
t	time
u	specific internal energy
$\boldsymbol{\sigma}$	Cauchy stress tensor
β	Taylor-Quinney coefficient
γ	entropy per unit volume
ε	total strain
θ	change in temperature
ρ	mass density
τ	time of one loading cycle
ψ	Helmholtz free energy

ORCID

Zhenjie Teng https://orcid.org/0000-0003-0305-9094

REFERENCES

1. Schütz W. A history of fatigue. *Eng Fract Mech*. 1996;54(2):263-300.
2. Schijve J. *Fatigue of Structures and Materials*. Dordrecht, Boston: Kluwer Academic Publ; 2001.
3. Boller C, Chang FK, Fujino Y. *Encyclopedia of Structural Health Monitoring*. John Wiley & Sons; 2009.
4. Lematre J, Dufailly J. Damage measurements. *Eng Fract Mech*. 1987;28(5-6):643-661.
5. Zhu SP, Hao YZ, De Oliveira Correi JAF, Lesiuk G, De Jesus AMP. Nonlinear fatigue damage accumulation and life prediction of metals: a comparative study. *Fatigue Fract Eng Mater Struct*. 2019;42(6):1271-1281.
6. Rotem A. Residual strength after fatigue loading. *Int J Fatigue*. 1988;10(1):27-31.
7. Ye DY, Wang ZL. An approach to investigate pre-nucleation fatigue of cyclically loaded metals using Vickers microhardness tests. *Int J Fatigue*. 2001;23(1):85-91.
8. Ye DY, Wang ZL. A new approach to low-cycle fatigue damage based on exhaustion of static toughness and dissipation of cyclic plastic strain energy during fatigue. *Int J Fatigue*. 2001;23:679-687.
9. Kocanda S. *Fatigue Failure of Metals*. Amsterdam: Elsevier; 1986.
10. Miner MA. Cumulative damage in fatigue. *J Appl Mech*. 1945;12:159-164.
11. Smith KN, Watson P, Topper TH. A stress-strain function for the fatigue of materials. *J Mater*. 1970;5:767-778.
12. Morrow J. Fatigue properties of metals, section 3.2. In: *Fatigue Design Handbook, Pub. No. AE-4*. Warrendale, PA: SAE; 1968.
13. Vormwald M, Heuler P, Seeger T. A fracture mechanics based model for cumulative damage assessment as part of fatigue life prediction. In: Mitchell MR, Landgraf RW, eds. *Advances in Fatigue Life Prediction Techniques*. Philadelphia, STP 1122: San Francisco American Society for Testing and Materials; 1992.
14. Haibach E. *Betriebsfeste Bauteile. Ermittlung und Nachweis der Betriebsfestigkeit, Konstruktive und Unternehmerische Gesichtspunkte*. Berlin: Springer Verlag; 1992.
15. Radaj D, Vormwald M. *Ermüdungsfestigkeit*. Berlin, Heidelberg: Springerverlag; 2007.
16. Chaboche JL, Lesne PM. A non-linear continuous fatigue damage model. *Fatigue Fract Eng Mater Struct*. 1988;11(1):1-17.
17. Shang DG, Yao WX. A nonlinear damage cumulative model for uniaxial fatigue. *Int J Fatigue*. 1999;21(2):187-194.
18. Benkabouche S, Guechichi H, Amrouche A, Benkhettab M. A modified nonlinear fatigue damage accumulation model under multiaxial variable amplitude loading. *Int J Mech Sci*. 2015;100:180-194.
19. Rege K, Pavlou DG. A one-parameter nonlinear fatigue damage accumulation model. *Int J Fatigue*. 2017;98:234-246.
20. Zhu SP, Liao D, Liu Q, Correi JAFO, De Jesus AMP. Nonlinear fatigue damage accumulation: isodamage curve-based model and life prediction aspects. *Int J Fatigue*. 2019;128:105185.
21. Bhattacharya B, Ellingwood B. Continuum damage mechanics analysis of fatigue crack initiation. *Int J Fatigue*. 1998;20(9):631-639.
22. Bryant MD, Khonsari MM, Ling FF. On the thermodynamics of degradation. *Proc R Soc A*. 2008;464(2096):2001-2014.
23. Basaran C, Nie S. An irreversible thermodynamics theory for damage mechanics of solids. *Int J Damage Mech*. 2004;13(3):205-223.
24. Naderi M, Khonsari MM. An experimental approach to low-cycle fatigue damage based on thermodynamic entropy. *Int J Solids Struct*. 2010;47(6):875-880.
25. Liakat M, Khonsari MM. An experimental approach to estimate damage and remaining life of metals under uniaxial fatigue loading. *Mater Des*. 2014;57:289-297.
26. Sun YJ, Hu LS. Assessment of low cycle fatigue life of steam turbine rotor based on a thermodynamic approach. *J Eng Gas Turbines Power*. 2012;134, 064504:1-4.
27. Amiri M, Naderi M, Khonsari MM. An experimental approach to evaluate the critical damage. *Int J Damage Mech*. 2011;20(1):89-112.
28. Karimian SF, Bruck HA, Modarres M. Thermodynamic entropy to detect fatigue crack initiation using digital image correlation, and effect of overload spectrums. *Int J Fatigue*. 2019;129:105256.

29. Salimi H, Pourgol-Mohammad M, Yazdani M. Metal fatigue assessment based on temperature evolution and thermodynamic entropy generation. *Int J Fatigue*. 2019;127:403-416.
30. Ontiveros V, Amiri M, Kahirdeh A, Modarres M. Thermodynamic entropy generation in the course of the fatigue crack initiation. *Fatigue Fract Eng Mater Struct*. 2017;40(3):423-434.
31. Teng ZJ, Wu HR, Boller C, Starke P. Thermography in high cycle fatigue short-term evaluation procedures applied to a medium carbon steel. *Fatigue Fract Eng Mater Struct*. 2020;43(3):515-526.
32. Jang JY, Khonsari MM. On the evaluation of fracture fatigue entropy. *Theor Appl Fract Mec*. 2018;96:351-361.
33. Horstemeyer MF, Bammann DJ. Historical review of internal state variable theory for inelasticity. *Int J Plasticity*. 2010;26(9):1310-1334.
34. Lemaitre J, Chaboche JL. *Mechanics of Solid Materials*. 1st ed. Cambridge, UK: Cambridge University Press; 1990.
35. Ribeiro P, Petit J, Gallimard L. Experimental determination of entropy and exergy in low cycle fatigue. *Int J Fatigue*. 2019;136:105333.
36. Morrow JD. Cyclic plastic strain energy and fatigue of metals. In: *Internal Friction, Damping, and Cyclic Plasticity*. *ASTM STP*. 1965;378:45-87.
37. Naderi M, Khonsari MM. A thermodynamic approach to fatigue damage accumulation under variable loading. *Mater Sci Eng A*. 2010;527(23):6133-6139.
38. Audenino AL, Crupi V, Zanetti EM. Correlation between thermography and internal damping in metals. *Int J Fatigue*. 2003;25(4):343-351.
39. Curà F, Gallinatti AE, Sesana R. Dissipative aspects in thermographic methods. *Fatigue Fract Eng Mater Struct*. 2012;35(12):1133-1147.
40. Risitano A, Risitano G. Cumulative damage evaluation in multiple cycle fatigue tests taking into account energy parameters. *Int J Fatigue*. 2013;48:214-222.
41. Wang XG, Crupi V, Jiang C, Guglielmino E. Quantitative thermographic methodology for fatigue life assessment in a multiscale energy dissipation framework. *Int J Fatigue*. 2015;81:249-256.
42. Knobbe H, Starke P, Hereñú S, Christ HJ, Eifler D. Cyclic deformation behaviour, microstructural evolution and fatigue life of duplex steel AISI 329 LN. *Int J Fatigue*. 2015;80:81-89.
43. He C, Liu YJ, Fang DH, Wang QY. Very high cycle fatigue behavior of bridge steel welded joint. *Theor App Mech L*. 2012;2(3):031010.
44. He C, Tian RH, Liu YJ, Li JK, Wang QY. Ultrasonic fatigue damage behavior of 304L austenitic stainless steel based on micro-plasticity and heat dissipation. *J Iron Steel Res Int*. 2015;22(7):638-644.
45. Liu HQ, Wang QY, Huang ZY, Teng ZJ. High-cycle fatigue and thermal dissipation investigations for low carbon steel Q345. *Key Eng Mater*. 2016;664:305-313.
46. Micone N, Waele W. On the application of infrared thermography and potential drop for the accelerated determination of an S-N curve. *Exp Mech*. 2017;57(1):143-153.
47. Wu HR, Bäumchen A, Engel A, Acosta R, Boller C, Starke P. SteBLife—a new short-time procedure for the evaluation of fatigue data. *Int J Fatigue*. 2019;124:82-88.
48. Boulanger T, Chrysochoos A, Mabru C, Galtier A. Calorimetric analysis of dissipative and thermoelastic effects associated with the fatigue behavior of steels. *Int J Fatigue*. 2004;26(3):221-229.
49. Wang XG, Feng ES, Jiang C. A microplasticity evaluation method in very high cycle fatigue. *Int J Fatigue*. 2017;94:6-15.
50. Fan JL, Zhao YG, Guo XL. A unifying energy approach for high cycle fatigue behavior evaluation. *Mech Mater*. 2018;120:15-25.
51. Farren WS, Taylor GI. The heat developed during plastic extension of metals. *Proc Roy Soc Lond A*. 1925;107:422-451.
52. Taylor GI, Quinney H. The latent energy remaining in a metal after cold working. *Proc Roy Soc Lond A*. 1934;143(849):307-326.
53. Eifler D, Piotrowski A. Bewertung zyklischer Verformungsvorgange metallischer Werkstoffe mit Hilfe mechanischer, thermometrischer und elektrischer Messverfahren. *Mat-Wiss U Werkstofftech*. 1995;26(3):121-127.
54. Rosakis P, Rosakis AJ, Ravichandran G, Hodowany J. A thermodynamic internal variable model for the partition of plastic work into heat and stored energy in metals. *J Mech Phys Solids*. 2000;48(3):581-607.
55. Guo Q, Guo XL, Fan JL, Syed R, Wu CW. An energy method for rapid evaluation of high-cycle fatigue parameters based on intrinsic dissipation. *Int J Fatigue*. 2015;80:136-144.
56. Spittel M, Spittel T. In: Warlimont H, ed. *Metal Forming Data of Ferrous Alloys-Deformation Behavior. Steel Symbol/Number: C45/1.0503*. Berlin, Heidelberg: Springer-Verlag; 2009:210-215.

How to cite this article: Teng Z, Wu H, Boller C, Starke P. Thermodynamic entropy as a marker of high-cycle fatigue damage accumulation: Example for normalized SAE 1045 steel. *Fatigue Fract Eng Mater Struct*. 2020;43:2854–2866. https://doi.org/10.1111/ffe.13303